

Microreaction for Microfuel Processing: Challenges and Prospects

Keyur Shah¹, X. Ouyang^{1,2}, and R.S. Besser¹

¹New Jersey Center for Microchemical Systems
Department of Chemical, Biomedical and Material Engineering
Stevens Institute of Technology
Castle Point on Hudson
Hoboken, NJ 07030

²Current address:

Laboratory of Genius of the Catalytic Processes (LGPC)- Centre National de la
Recherche Scientifique (CNRS)
Lyon School of Chemistry, Physics and Electronic (CPE Lyon)
43 bd du 11 Nov 1918, BP 2077
69616 Villeurbanne, France

Correspondence:

Ronald S. Besser
Department of Chemical, Biomedical, and Materials Engineering
Stevens Institute of Technology
Castle Point on Hudson
Hoboken, NJ 07030
(201) 216-5257 (voice)
(201) 216-8306 (fax)
rbesser@stevens.edu

Abstract

The processing of high density liquid hydrocarbon fuels appears to be the most promising method of supplying a hydrogen stream for feeding portable fuel cells. Furthermore, microchemical systems are a strong enabling aspect of compact fuel processors due to their advantageous heat and mass transport and inherent compactness.

However, a number of crucial challenges exist for the realization of practical fuel processors. In this article, we delineate these challenges, and then show two examples of how the challenges can be attacked in the context of implementation of microchemical systems. The examples revolve around (a) appropriate measurement of kinetics in microchannel-catalyst systems with preferential oxidation of carbon monoxide as a model, and (b) thermal integration of reactor components with a methanol steam reformer as a model.

1. Introduction

Because of their size and portability, microchemical systems have shown promising results in chemical process miniaturization. The use of microreactor technology in the field of fuel processing to convert hydrocarbon fuels to hydrogen, for the production of electricity, is one such example. Microreaction can facilitate highly compact power sources through integration of a fuel cell (FC) with all the unit operation components of a fuel processor (FP) along with microstructured sensors, actuators and other “balance of plant” (BOP) devices.

As FCs gain more attention as potential energy sources to meet global demand and to reduce environmental pollution such as greenhouse gases [1,2], one of the most promising fields of application is portable power, as a prominent alternative to batteries. In applications where the power requirements are low but the weight and volume are critical, it is already clear that miniature FCs will be preferred over conventional batteries. High energy density is required for advanced portable applications for consumer use (e.g., laptop computers, cellular phones, medical and telecommunication devices), and also for military and intelligence use (e.g., computation, imaging, and communication devices; weaponry capabilities, and micro sensors and actuators to detect a variety of effects including chem-bio warfare agents), with the goal of allowing these devices to operate for longer times with less recharging. Even with recent progress, projections show that available energy density from lithium ion batteries may be inadequate [3,4]. The ever-increasing energy demand for consumer and military devices continues to stimulate research and development of compact FCs among several academic and corporate research groups.

The proton exchange membrane fuel cell (PEMFC) is particularly attractive and promising for portable applications because of its ability to provide instant power and simplicity in design and operation, allowing fabrication of a compact and lightweight cell, mild operating conditions (temperature less than 100°C, pressure in the range of a few atmospheres), and relatively low loading of precious metal catalysts [1,5,6].

The success of PEMFC technology for portable power depends heavily on the development of an efficient means of delivering the appropriate fuel to the cell. PEMFCs operating on hydrogen as the fuel give the best possible efficiency and power density [7,8]. However, since gaseous hydrogen is difficult to store because of its low compressibility, some other high energy density storage method is required such as metal hydrides, highly pressurized cylinders, or possibly carbon nanotubes [9-11]. To overcome this obstacle, two main alternatives are commonly envisioned and employed for portability. One approach, the direct methanol fuel cell (DMFC), employs methanol directly in the cell to generate electricity. Several groups are seriously pursuing low power DMFCs for portable power applications. R. Dillon et al. [12] have summarized the worldwide research and development activities being carried out in the field of DMFC technology development. However, low power density and methanol crossover are persisting challenges that currently limit the DMFC to less stringent applications.

The other, higher performance alternative, generating pure hydrogen by processing easily stored liquid fuels represents an attractive source of hydrogen [13,14]. Fuel processing adds complexity, weight, and cost compared to the DMFC or a system running directly on hydrogen, however the effective energy storage density is high.

Liquid hydrocarbons could quickly become a viable energy source for portable power if an efficient, lightweight, and portable FP/FC integrated system were made available.

Considerable efforts are being made to develop such an integrated system; however there are major hurdles and several universal challenges exist. Based on the literature and research conducted by our group, several of the key issues observed with fuel processing at small scale are the following:

1) **System complexity and packaging.** Fuel processing of liquid hydrocarbons needs several unit operations and process steps to supply high purity hydrogen. Optimally, each component of a micro FP should be designed with the goal of miniaturization in mind instead of simply scaling down larger systems. Further, the fuel processing unit should be holistically integrated with the BOP, the fuel delivery system, and a micro FC stack. This demands a system level view of miniaturization and appropriate physical integration of all of the above components.

2) **Kinetics evaluation for each unit operation.** When using a microreactor and a compatible catalyst technology for a gas-phase reaction at low temperature, often mass transport effects are negligible and hence intrinsic kinetics dominate. However, this is not always the case. A detailed study of kinetics is required for the correct sizing of reactor components and to obtain desirable operating conditions for optimum performance. The dependence of kinetics with temperature tends to be the dominant factor in sizing and integration and must be clearly established. Furthermore, the catalyst performance (activity, selectivity, and stability) should be verified under realistic conditions through experimental reaction kinetics studies.

3) **Heat management.** The management of heat in a compact format is perhaps the most crucial challenge for micro scale FPs. High thermal efficiency can be achieved by coupling endothermic and exothermic components and minimizing losses. However, such coupling must be accomplished in a manner that permits the maintenance of specific temperatures in the various components and maintains the surface of the package near room temperature. Novel thermal insulation schemes thus need to be explored that can meet these demands with minimal added weight and volume.

4) **Miniature BOP components.** The currently available BOP components like valves, pumps, fans, sensors, actuators, etc., are too large for small, low-power systems and require considerable reduction in size, weight, and power consumption, as well as the ability to integrate them in a variety of materials approaches. Further, it is necessary to develop miniaturized embedded control systems. Thus, new technologies that could make it possible for example, to seamlessly integrate Si micro sensors and actuators with robust stainless steel reactor modules are highly desired.

5) **Water management.** The FP/FC is a net water producing system. The reforming process requires water while water can be recovered from the FC and recycled back to the reformer, which would obviate the need for separate storage. However, the complexity of separate water lines and associated sensor and control units may offset the benefits of recycling.

6) **Internal energy demand.** The catalytic combustion of the unconverted hydrogen from the anode of the FC is usually carried out to provide energy necessary for fuel and water vaporization and superheat as well as for the endothermic SR reaction. If the FC is operated at high hydrogen flows, the residual hydrogen may be insufficient to

supply this energy. In this case the hydrocarbon fuel would be used by the combustor. Providing for various internal fueling combinations will require increasing levels of complexity in system design and control.

7) **Dynamic control.** The total design must consider startup demand, peak and partial power demands, and power required to drive the BOP components. An on-board rechargeable battery can provide initial power for start up and for peak power periods. Rapid thermal equilibration will be aided by the low thermal mass and high transport rates characteristic of microsystems; the integration scheme must be chosen to minimize negative impact on these beneficial attributes.

8) **Fate of exhaust gases.** The post-reforming clean up steps will effectively eliminate carbon monoxide (CO) from the system. Exhaust gases from the combustor may be fed through clean up reactors or safely released into the atmosphere if CO levels are low enough. Separate waste stream clean up, should it be necessary, will add complexity.

2. Background

2.1 Generating Hydrogen from Hydrocarbons

Promising alternatives to batteries as portable power sources can be identified by a comparison of energy densities. Table 1 shows the energy density of available primary and secondary batteries [15] compared with the energy density stored in several pure hydrocarbons.

While a wide variety of hydrocarbons such as natural gas, methanol, gasoline, and diesel can be reformed into hydrogen-rich streams, the choice of hydrocarbon and method

used to produce the hydrogen play a major role in the design of a FP system. Conversion of liquid hydrocarbons involves a series of steps including fuel vaporization, reforming (three main processes available are partial oxidation, steam reforming, and autothermal reforming), water gas shift (WGS), and CO clean up (by preferential oxidation (PrOx) to CO₂, hydrogen separation by permeation through a hydrogen-selective membrane or pressure swing adsorption method) before feeding hydrogen rich gases to the FC.

Methanol (CH₃OH) is an attractive fuel for portable power, offering high hydrogen-carbon ratio, high energy density (5600 Wh/kg), ready availability, and low boiling point [16]. Moreover, methanol is sulfur free and can be reformed relatively easily at low temperatures (250-300°C), simplifying the micro FP design. Figure 1 shows a schematic for processing of methanol to produce hydrogen-rich gas suitable for a low temperature (70-80°C) PEMFC.

The steam reforming reaction is highly endothermic in nature and thus requires external energy. However, this energy can be reasonably met by the hydrogen in the anode exhaust. A relatively low CO concentration of 1-2% is attained while operating the reformer at temperatures ranging from 220–260°C as a consequence of reaction thermodynamics [17-20]. Therefore, a methanol-based fuel processing system must include a CO clean up step, as this relatively low level of CO is still sufficient to poison the PEMFC catalyst. However, the CO concentration of only a few percent eliminates the need for a separate WGS step, requiring only the PrOx to reduce CO below 10 ppm.

2.2. Applications of Microreactor Technology to Micro FP Design

The demand for a greater energy per volume and weight has naturally led to the investigation of microreactors which can take the form of any of the essential FP

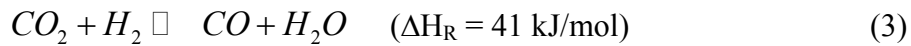
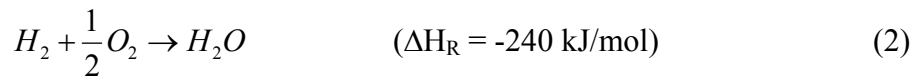
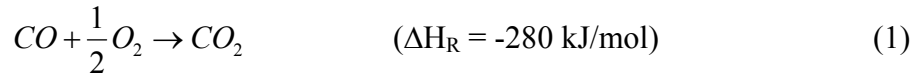
elements including desulfurizer, steam reformer (SR), PrOx reactor, etc. Microchemical systems seem suited to small-scale power generation as their compactness should enable integration by stacking of miniature FP and FC components with the fuel delivery system [21]. The microscale dimensions which result in extremely small transport resistances [22,23], make them especially attractive in applications where it is necessary to efficiently thermally couple highly endothermic and exothermic processes. The excellent transport properties further ensure a fast response time, which is necessary for start up and transient operation. With the advances in microsystem technology, it is possible to have precise control over geometry of the fluidic structures resulting in a well-defined distribution of residence time [24].

Several groups are working on research and development of metal [25-30], silicon [31-34], and ceramic [35] based microreactor components of a portable FP. Major research efforts are pursued to develop and improve microreactors for in situ methanol reforming [25,28,31,34], as a critical component of a micro FP. While a variety of materials approaches have emerged, all these approaches are confronted with most of the crucial challenges listed above.

In order to understand the relationships and tradeoffs of the crucial system issues listed in the above section, we performed a system study encompassing energy density, heat management, component sizing, and integration. We present in the next major sections, how two of the limitations above are being addressed through research in our lab.

3. Kinetic Evaluation: Preferential Oxidation of CO

The need for reliable kinetic information of the unit reaction processes is essential for robust design of micro FP systems. The development of novel catalyst approaches for microchannel systems makes the acquisition of kinetic data a practical necessity as opposed to simply using literature rate laws developed for materials prepared by traditional methods. As a model case of this crucial issue, we focus on the determination of relevant kinetics for the PrOx reaction (Eq. (1)) and relevant side reactions (Eqs. (2) and (3)).



The reaction kinetics of PrOx on Pt/Al₂O₃ has been extensively studied in the literature due to its proven effectiveness. However, most of these studies were carried out in conventional minimized packed-bed lab reactors (m-PBRs) and the intrinsic kinetics could be hidden by the mass and heat transport limitations. A silicon microchannel reactor with Pt/Al₂O₃ thin-film wall catalyst was thus adopted in our study to gain direct access to PrOx reaction kinetics as well as to study the catalyst behavior under conditions close to the final intended microchannel implementation. In order to quantitatively study intrinsic reaction kinetics and the effect of transport limitations on kinetic assessment, a comprehensive method, integrating transport limitation evaluation, microkinetic reaction simulation, and 3D non-isothermal reactor design, was developed.

Pt/Al₂O₃ has been the most studied PrOx catalyst because of its high CO conversion and stability at moderate temperatures (~200 °C) [36-38]. Other noble metals, metal oxide, and bimetallic catalysts have also received attention [39-45]. Preparation and pretreatment methods have been considered as another route to gain better catalytic activity by affecting material structure and particle size [46-48].

Until now, most PrOx studies [36,38,39,41,42,43,44] have been based on m-PBRs, and are thus subject to the limitations imposed by them [49,50]. Therefore, practical PrOx reactor designs often adopt small catalyst particles to reduce transport resistance [40] and multi-stage reactors [51] to gain better thermal management. The drawback of adopting small particles is the increase of pressure drop while the multi-stage reactor systems increase overall system size, complexity, and above all, packaging and operation cost. The advantages of microreactors [22,23,52], especially their enhanced mass and heat transport properties, make them promising candidates for PrOx reactors and an ideal tool for intrinsic reaction kinetic studies.

3.1 Heat and Mass Transport Limitations

We first examined existing criteria for mass transport and heat transport limitations for both the microreactor (with a thin-film wall catalyst thickness of 5 μm) and the m-PBRs (with radii of 2 and 4 mm) [53]. We found that within typical PrOx operating temperatures (160 ~ 220°C), both types of reactor show negligible internal and external mass transport resistance. On the other hand, an estimate of the *Damköhler (Da)* number for intraparticle heat transport indicated strong limitations for the m-PBR in which the catalyst thickness (t_{cat}) is the determining factor. The t_{cat} of the thin-film catalyst (5x10⁻⁶ m) of the microreactor is orders of magnitude smaller than that for the

packed-bed catalyst ($\sim 2 \times 10^{-3}$ m) of m-PBR. Due to the quadratic dependence of Da on the t_{cat} , Da of the m-PBR with 2×10^{-3} m radius (2-mm m-PBR) is more than 5 orders of magnitude of Da for the microreactor. The Mear's criterion [53] then suggests severe heat transport limitations for the m-PBR for the highly exothermic PrOx reaction.

3.2 Microkinetic Reaction Simulation

A microkinetic reaction model was formed to understand the intrinsic reaction mechanism and to provide insight into the processes occurring in the reactor. The CHEMKIN[®] software [54], an integrated software package for modeling complex chemical kinetic processes, was used (in collaboration with Reaction Design, Inc.) to adapt this model. The PrOx reaction mechanism describing the detailed gas phase and surface chemical kinetics was constructed by extracting the relevant reactions from previously published work [55] and altering the rate parameters for the oxygen adsorption reaction in order to reproduce our experimental results. As shown in Table 2, the model includes 8 adsorption reactions (reactions 1 – 8), 8 desorption reactions (reactions 9 – 16) and 12 surface reactions (reactions 17 – 28) involving 9 gas-phase species and 8 surface species. A reaction network (Figure 2) that comprises the reaction pathways for consumption of CO and formation of H₂O and CO₂ was then created to analyze the importance and sensitivity of each elementary reaction on overall reaction activity. The model was verified by experimental comparison of effects of O₂ adsorption [36,38,45,56], effect of surface hydroxyl [57,58], and effect of hydrogen in the feed [36,45,46,56,57,59,60]. With verification of the above reaction mechanisms, the CHEMKIN model was then used to predict the experimental results of CO conversion and CO₂ selectivity in the microreactor [Figure 3], and good agreement was attained [53].

The combination of experimental studies and detailed chemical kinetic simulations corroborated key reaction mechanisms and more importantly, provided a more complete picture of surface kinetics while increasing the efficiency of experiment design.

3.3 *Quasi-3D Non-Isothermal Reactor Model*

The PrOx studies based on m-PBR with particulate catalyst almost universally found a narrow operating temperature window for CO conversion [36,37,40], followed by the decline of both CO conversion and CO₂ selectivity with further temperature increase. In contrast, our studies with microreactors showed essentially 100% CO conversion between 180°C and 280°C while there is only a slight drop-off (< 1%) at 300°C, suggesting a much wider operating window for CO conversion (Figure 4). Other investigations [39,56,61] found that this falloff is caused by the reverse water gas shift (r-WGS) reaction (Eq. (3)), the effect of which becomes more pronounced in the presence of temperature non-uniformities. Due to the fast surface chemistry of the exothermic CO oxidation and H₂ oxidation and the comparatively low thermal conductivity of the catalyst material, reaction heat can accumulate within the packed-bed, leading to an uneven temperature distribution and higher local temperatures (hot spots) in the reactor. This heat accumulation becomes more severe with the increase of the catalyst thickness (t_{cat}) according to Mear's criterion, which activates the endothermic r-WGS reaction and eventually limits the net CO conversion.

In order to further assess the effects of heat transport limitations on PrOx kinetic behavior and to compare these effects for both the microreactor and the m-PBR, we constructed a quasi-3D non-isothermal reactor model coupled with the reaction kinetics of all major PrOx reactions (i.e., Eqs. (1), (2), and (3)) [62]. A finite difference method

was adopted to calculate the 3D temperature distribution inside the reactor. The 3D modeling is necessary since both axial and radial temperature gradients can form as indicated in our heat transport evaluation with Mear's criterion.

Simulations were done for a microreactor of 5- μm catalyst thickness and m-PBRs of two different radii (2-mm and 4-mm), with identical reactor length for both types of reactors. In this model, cylindrical geometry was used to approximate both the microchannel and the packed bed. Thus the 3D reactor structure can be represented by the quasi-3D finite difference grid in radial and axial directions. With the kinetic expressions [38,50,61] and parameters evaluated by our experimental data, reactant concentrations and temperature were calculated at each grid point, assuming identical boundary temperature and weight hourly space velocity (*WHSV*) for both cases.

Supporting the Mear's criterion calculation result, the modeling results of the microreactor showed essentially isothermal temperature distribution in the thin-film catalyst even at the highest operating temperature (300°C). Also as predicted, the results for the 2-mm m-PBR indicated significant temperature gradients and effect on PrOx performance, as shown in Figure 5 with the 3D temperature profile at three representative wall temperatures ($T_w = 120^\circ\text{C}, 180^\circ\text{C}, 220^\circ\text{C}$).

Figure 6 plots the modeling results of CO conversion at different wall temperatures for the microreactor and m-PBRs with 2×10^{-3} m and 4×10^{-3} m radii (2-mm and 4-mm m-PBRs), all with the same *WHSV* (1500 hr^{-1}) and isothermal wall temperatures. The CO conversion curve for the microreactor essentially coincides with the result for ideal isothermal operation. On the contrary, the CO light-off curves for the m-PBRs' shift to lower temperatures and CO conversion drops significantly at higher

wall temperatures. The light-off shift to lower temperature is due to an increase in CO oxidation rate at local hot spots. With further temperature increase, however, these temperature non-uniformities activate the r-WGS reaction, leading to a drop of net CO conversion. This phenomenon intensifies as the radial thermal resistance increases (4-mm vs. 2-mm). The inability of the 4-mm m-PBR to reach 100% conversion is indicative of severe hot spots even at relatively low wall temperatures. The CO conversion curves from literature PrOx studies with m-PBR [36,38,39] agree qualitatively with these modeling results and thus can be understood with the above discussion.

Overall, the m-PBRs have severe temperature gradients with the activation of exothermic CO and H₂ oxidation reactions, leading to significant r-WGS reaction activity. In contrast, the isothermality within the microreactor effectively removes the reaction heat and minimizes the extent of the r-WGS side reaction. The sensitivity of PrOx performance on temperature brings attention to thermal management in the design of practical reactors. In addition, the thin-film catalyzed microreactor was shown to be an ideal kinetic tool for highly exothermic reactions by suppressing temperature non-uniformities and allowing more direct access to intrinsic kinetics.

4. Example of Heat Management: Development of an Integrated Micro SR

Catalytic steam reforming of methanol on a metal oxide catalyst (usually CuO/ZnO-based) is a highly efficient process, producing a reformat with high hydrogen concentration (65-70%) while maintaining high CO₂ selectivity compared to other available reforming processes.

The following chemical reactions take place during the reforming process.



Eq. (4) is the main reforming reaction and Eq. (5) is the undesired methanol decomposition reaction, while Eq. (6) represents the WGS reaction, the activity of which helps reduce CO level with the added benefit of liberating H₂ from the H₂O feed.

A quasi two-dimensional thermal model was formulated as shown in Figure 7 to determine favorable thermal integration of the combustor with the SR and vaporizer using the literature kinetic expressions [63,64] in combination with an energy balance derived for the system. The combustor emits energy which is used to heat the endothermic SR microreactor and to evaporate and superheat the methanol-water feed to 260°C in a microchannel vaporizer. These kinetic and energy balance equations were solved to determine temperature profiles along the axial length of combustor, SR, and vaporizer using a fourth order Runge-Kutta algorithm in MATLAB®. For generality, the model did not consider heat losses.

Different SR, combustor, and vaporizer arrangements were analyzed. The best results are obtained with a stacking arrangement having cocurrent flow between the combustor and SR streams and countercurrent flow between the vaporizer and combustor streams. Figure 7 shows the temperature profiles along the length of these components for this stacking arrangement and the conditions given in the caption. The catalytic combustion of hydrogen is very fast at the entrance of reactor, releasing large amount of heat. Therefore, cocurrent flow configuration of SR and combustor is desirable to take

advantage of the high temperature driving force at the inlet to the SR, where the endothermic rate of reaction is greatest. Counter flow of the vaporizer stream allows utilization of the sensible heat in the combustor effluents.

Since details of the analysis revealed that the SR is the most critical component of the FP, a subsequent objective was to design, fabricate, and demonstrate a silicon microreactor-based SR in the context of complete thermal integration as determined from the simulations for the overall system.

Because of several advantages, we are employing silicon for microreactor fabrication, specifically the ability to create novel microchannel and reactor configurations in the sub-millimeter range with tight dimensional controls. Silicon is 2-3 times lighter than stainless steel; it possesses high mechanical strength, chemical inertness, thermal stability, and large thermal conductivity. An important advantage of silicon microfabrication is its compatibility with thin film technology. This facilitates eventual on-chip integration of functional elements like sensors and actuators allowing compact process control subsystems, which would need to be constructed as external units for other materials approaches. However, it is our intent at this stage to perform experiments whose outcome depends most critically on microscale geometry and less so on the materials of construction. In this way the results obtained may be generalizable to any of the materials technologies.

4.1. Thermal Coupling and Insulation

The FP needs effective thermal coupling to allow transfer of energy from the heat producing combustor to the vaporizer and the endothermic SR. These three components operate at different temperatures and it is necessary to maintain desired temperatures in

each, most critically the SR. Therefore, heat management offers a dual challenge of opposing the heat losses from the system that arise from the high surface-to-volume ratio in tandem with maintaining temperature gradients within the system to allow desired conditions in the unit reaction steps. Because of the short conduction paths inherent to microreactors, only insulating materials that can offer ultra low thermal conductivity can be effective to bridge these temperature differences and to minimize conductive and convective heat losses to the surroundings.

The best commercial insulators have thermal conductivities in the range of 0.02 W/mK and are difficult to integrate into a microfabricated unit. However, vacuum packaging of microreactors can provide an effective means of insulation. From the kinetic theory of gases, it is known that the thermal conductivity of a gas is approximately independent of pressure for atmosphere and above [65], and decreases with sub-atmospheric pressures, as the mean free path becomes less than the enclosure dimensions [66]. A microfabricated cavity surrounding the reactor filled with low-pressure gas offers low thermal conductivity down to approximately 0.001 W/mK. Silicon microfabrication enables a straightforward approach to this structure. Figure 8 shows one concept for integrating vacuum insulation.

4.2. Integrated Micro SR: Design

The design of a test vehicle to simulate an integrated SR is shown in Figure 9, where vacuum packaging chips, thin film metal heaters and temperature sensors are directly embedded with the microreactor. Well defined external heat flux is introduced to simulate the flows that result from integration with other components. Distributed sensors are provided to obtain the temperature profiles along the axial length. Detailed thermal

data (heat input required, heat losses, temperature profiles) and reaction data (conversion and selectivity) are acquired and compared to the computational fluid dynamics (CFD) model for the system. The results from this test microreactor are expected to significantly expand understanding of the critical limitations imposed by SR in an overall integrated scheme. A refined understanding of SR behavior will then lead to a robust design of an integrated SR for 20 W_e .

The steam reforming reaction is relatively slow and hence needs an appropriate mass of catalyst at this temperature range to achieve high conversion. The preliminary size estimates based on a thin-film catalyst approach is unfavorably large for an SR microreactor at this scale, based on the achievable loading. Thus a new approach to incorporate catalyst into a microreactor at higher loading is needed. The concept of a foam-based cellular catalyst, offering significantly higher loading than thin-film catalysts, was chosen. Catalyst foams offer low-pressure drop compared to packed beds as they are highly porous and the pores are well interconnected [67,68].

Figure 8(d) shows the design of the SR microreactor test vehicle. This initial test reactor is suitable to produce enough hydrogen for 2.45 W_e as a demonstration tool.

4.3. Fabrication of an Integrated Test Vehicle

Two microreactors were fabricated on a single silicon wafer (p-type <100> 4 inch diameter, 650 micron thick) by silicon bulk micromachining techniques. Photolithography was employed first to pattern the front side of the microreactors using thick photoresist. These structures were then etched to a depth of 400 μm using deep reactive ion etching (DRIE) by inductively coupled plasma (ICP) [69]. A two-micron thick silicon dioxide hard mask was used for deep silicon etching. Once the front side

was processed, a second mask was used for backside patterning of inlet and outlet vias. These vias were then opened from the backside by wafer through-etching with DRIE. The fabricated wafers were diced into individual microreactors of size 4.0 cm × 4.0 cm as shown in Figure 8(e).

For the vacuum insulation, a square cavity was patterned on the silicon wafer and etched to a depth of 200 micron using DRIE. Thin film Pt heater and temperature sensors were fabricated on Pyrex™ glass wafers. A 10nm of Ti adhesion layer is deposited followed by 150nm of Pt using e-beam evaporation. These thin films were patterned by lift-off, leaving the Ti/Pt heater and temperature sensors as shown in Figure 10.

Next, the integrated device is packaged for fluidic and electrical connections. For the surrounding insulation parts, two Pyrex™ glass wafers patterned above with sensors and heater are bonded to enclose a vacuum cavity in Si. The bonded device is then diced into an individual insulation chip of 3 cm × 5 cm. The next step is to bond the bottom insulation chip with a silicon microreactor chip.

The catalyst is incorporated into the silicon microreactor and the reactor with bottom insulation part is then bonded with the glass cover and top insulation using a low temperature bonding method [70,71] as the SR catalyst can not withstand high bonding temperatures typical of the anodic bonding method (350-500 °C). Finally, the integrated steam reforming microreactor fabricated as above is characterized on a custom-built test setup. Results of these experiments now in progress will be published as they become available.

Conclusion

Microreaction technology appears to be a natural fit to the needs imposed by miniature FP systems. Development of a miniature chemical system that can effectively exploit the high energy density of methanol and other liquid hydrocarbons offers a number of significant technological challenges that we have enumerated in this paper.

Firstly, a comprehensive approach to understanding kinetic limitations was demonstrated for a PrOx system based on a microchannel with Pt/Al₂O₃ thin-film wall catalyst as a model. Secondly a Si microreactor-based catalytic SR was designed and fabricated in context of complete thermal integration to directly address the heat management issue.

To our knowledge, there has not yet been a demonstration of a standalone miniature FP/FC system integrated with BOPs. Design and demonstration of a compact, lightweight, and efficient micro FP seem possible with advances in microreaction technology. However, substantial ongoing research and development work are needed to realize a complete system.

Acknowledgements

The authors acknowledge the financial support from the Picatinny TACOM/ARDEC, Defense Advanced Research Project Agency (DARPA), and New Jersey Commission of Science and Technology (NJCST).

The silicon and glass microfabrication was performed in part at the Cornell NanoScale Facility (a member of the National Nanofabrication Users Network) which is supported by the National Science Foundation under Grant ECS-9731293, Cornell University and industrial affiliates.

Symbols used

Letters

$WHSV$	weight hourly space velocity, defined as mole of total reactant flow per mole of precious metal in the catalyst per hour (hr^{-1})
t_{cat}	effective interparticle heat conduction distance: catalyst thickness for the microreactor or reactor inner radius for m-PBR (m)
T_w	reactor inner wall temperature ($^{\circ}\text{C}$)
Da	Damkóhler's number for heat transport
ΔH_R	Reaction enthalpy

References

1. *Fuel Cell Handbook* (Eds: A. Appleby, F. Foulkes), Van Nostrand Reinhold, New York **1989**.
2. *Fuel Cell Handbook*, fifth ed., (Report prepared by EG&G Services for the US Department of Energy, National Energy Laboratory) October **2000**.
3. C.K. Dyer, *J. Power Sources* **2002**, 106 (1-2), 31.
4. M. Laurent, N. Ponath, J. Muller, *Fuel Cells Bulletin* **2001**, 4 (39), 9.
5. T. Thampan, S. Malhotra, J. Zhang, R. Datta, *Catal. Today* **2001**, 67, 15.
6. K. Kordesch, G. Simader, *Fuel Cells and Their Applications*, VCH, Germany **1996**.
7. D.G. Loffler, K. Tylor, D. Mason, *J. Power Sources* **2003**, 117 (1-2), 84.
8. B. Lindstrom, L.J. Pettersson, *J. Power Sources* **2003**, 118, 71.
9. Q. Ming, T. Healey, L. Allen, P. Irving, *Catal. Today* **2002**, 77, 51.
10. A. Ming, J. Wu, Q. Wang, *Int. J. Hydrogen Energy* **1995**, 20, 141.
11. S. Tony, V. Rangelova, N. Nikolay, *J. Alloys and Compounds* **2002**, 334(1-2), 219.
12. R. Dillon, S. Srinivasan, A.S. Arico, V. Antonucci, *J. Power Sources* **2004**, 127, 112.
13. C. Song, *Catal. Today* **2002**, 77, 17.
14. A.Y. Tonkovich, J.L. Zilka, M.J. LaMont, Y. Wang, R.S. Wegeng, *Chem. Eng. Sci.* **1999**, 54, 2947.
15. A. Girson, presented at *Sensors Expo and Conference*, MI, **2004**.
16. Y. Choi, H.G. Stenger, *Appl. Catal; B* **2002**, 38, 259.
17. J.C. Amphlett, M.J. Evans, R.A. Jones, R.F. Mann, R.D. Weir, *Can. J. Chem. Eng.* **1981**, 59, 720.
18. P.J. de Wild, M.J.F.M. Verhaak, *Catal. Today* **2000**, 60(1), 3.

19. B.A. Peppley, J.C. Amphlett, L.M. Kearns, R.F. Mann, *Appl. Catal; A* **1999**, 179, 21.
20. C.J. Jiang, D.L. Trimm, M.S. Wainwright, *Appl. Catal; A* **1993**, 93, 245.
21. W. Ehrfeld, V. Hessel, and H. Lowe, *Microreactors: New Technology for Modern Chemistry*, Wiley-VCH, Weinheim **2000**.
22. R.S. Besser, X. Oyuang, H. Surangalika, *Chem. Eng. Sci.* **2003**, 58, 19.
23. H. Surangalika, X. Ouyang, R.S. Besser, *Chem. Eng. J.* **2003**, 93, 217
24. R.S. Besser, *Chem. Eng. Comm.* **2003**, 190, 1.
25. J.D. Holladay, E.O. Jones, M. Phelps, J. Hu, *J. Power Sources* **2002**, 108, 21.
26. D.R. Palo, J.D. Holladay, R.T. Rozmiarek, C.E. Guzman-Leong, Y. Wang, J. Hu, Y. Chin, R.A. Dagle, E.G. Baker, *J. Power Sources* **2002**, 108, 28.
27. J. Hu, Y. Wang, D. Vanderwiel, C. Chin, D. Palo, R. Rozmiarek, R. Dagle, J. Cao, J. Holladay, E. Baker, *Chem. Eng. J.* **2003**, 93, 55.
28. D. Seo, W. Yoon, Y. Yoon, S. Park, G. Park, C. Kim, *Electrochim. Acta* **2004**, 50, 719.
29. E.R. Delsman, M.H.J.M. de Croon, G.J. Kramer, P.D. Cobden, Ch. Hofmann, V. Cominos, J.C. Schouten, *Chem. Eng. J.* **2004**, 101(1-3), 123.
30. E.R. Delsman, E.V. Rebrov, M.H.J.M. de Croon, J.C. Schouten, in *Proc. of the 5th International Conference on Microreaction Technology* (Eds: M. Matlosz, W. Ehrfeld, J.P. Baselt), Springer Verlag, Berlin, Germany **2001**.
31. A.V. Pattekar, M.V. Kothare, *Journal of Microelectromechanical system* **2004**, 13(1), 7.
32. S.V. Karnik, M.K. Hatalis, M.V. Kothare, *Journal of Microelectromechanical System* **2003**, 12, 93.

33. L.R. Arana, S.B. Schaevitz, A.J. Franz, M.A. Schmidt, K.F. Jensen, *Journal of Microelectromechanical System* **2003**, 12(5), 1.
34. S. Tanaka, J.S. Chang, K. Min, D. Satoh, K. Yoshida, M. Esashi, *Chem. Eng. J.* **2004**, 101(1-3), 143.
35. J.A. Hallmark presented at *The Knowledge Science Foundation's 5th Int. Small Fuel Cells 2003: Small Fuel Cells for Portable Power Applications*, New Orleans, LA, **May 2003**.
36. M.J. Kahlich, H.A. Gasteiger, R.J. Behm, *J. Catal.* **1997**, 171, 93.
37. G.S. Zafiris, R.J. Gorte, *J. Catal.* **1993**, 140, 418.
38. Y. Choi, H.G. Stenger, *J. Power Sources* **2004**, 129, 246.
39. S.H. Oh, R.M. Sinkevitch, *J. Catal.* **1993**, 142, 254.
40. T.V. Choudhary, D.W. Goodman, *J. Catal.* **2002**, 207, 247.
41. O. Korotkikh, R. Farrauto, *Catal. Today* **2000**, 62, 249.
42. X. Liu, O. Korotkikh, R. Farrauto, *Appl. Catal. A* **2002** 226, 293.
43. G.W. Roberts, P. Chin, X.L. Sun, J.J. Spivey, *Appl. Catal, B* **2003**, 46, 601.
44. Y. Teng, H. Skurai, A. Ueda, T. Kobayashi, *Int. J. Hydrogen Energy* **1999**, 24(4), 355.
45. G. Avgouropoulos, T. Ioannides, Ch. Papadopoulou, J. Batista, S. Hocevar, H.K. Matralis, *Catal. Today* **2002**, 75, 157.
46. I.H. Son, M. Shamasuzzoha, A.M. Lane, *J. Catal.* **2002**, 210, 460.
47. I.H. Son, A.M. Lane, D.T. Johnson, *J. Power Sources* **2003**, 124, 415.
48. C. Serre, F. Garin, G. Belot, G. Maire, *J. Catal.* **1993**, 141, 9.
49. S.K. Ajmera, C. Delattre, M.A. Schmidt, K.F. Jensen, *J. Catal.* **2002**, 209, 401.

50. D.H. Kim, M.S. Lim, *Appl. Catal. A* **2002**, 224, 27.
51. S.H. Lee, J. Han, K.Y. Lee, *J. Power Sources* **2002**, 109, 394.
52. G. Kolb, V. Hessel, *Chem. Eng. J.* **2004**, 98, 1.
53. X. Ouyang, L. Bednarova, P. Ho, R.S. Besser, *AIChE J*; in press.
54. R.J. Kee, F.M. Rupley, J.A. Miller *et al.*, *Chemkin Collection, Release 3.7.1*. San Diego, CA, Reaction Design, Inc; **2003**.
55. D.K. Zerkle, M.D. Allendorf, M. Wolf, O. Deutschmann, *J Catal.* **2000**, 196, 18.
56. A. Manasilp, E. Gulari, *Appl. Catal. B.* **2002**, 37, 17.
57. M.M. Schubert, H.A. Gasteiger, R.J. Behm, *J. Catal.* **1997**, 72, 256.
58. A.B. Mhadeshwar, D.G. Vlachos, *J. Phys. Chem. B* **2004**, 108, 15246.
59. O. Korotkikh, R. Farrauto, *Catal. Today* **2000**, 62, 249.
60. R.H. Nibbelke, M.A.J. Campman, J.H.B.J. Hoebink, G.B. Marin, *J Catal.* **1997**, 171, 358.
61. R.H. Venderbosch, W. Prins, W.P.M. van Swaaij, *Chem. Eng. Sci.* **1998**, 53, 3355.
62. X. Ouyang, R.S. Besser, *J. Power Sources.*, in press.
63. S.R. Samms, R.F. Savinell, *J. Power Sources* **2002**, (112), 13.
64. R.W. Schefer, *Combust. Flame* **1982**, 45, 171.
65. F.P. Incropera, D.P. Dewitt, *Fundamental of Heat and Mass Transfer*, 5th ed., John Wiley & Sons, NY **2001**.
66. P. Atkins, J.D. Paula, *Physical Chemistry*, 7th ed., W.H. Freeman & Company, NY **1997**.
67. J.T. Richardson, Y. Peng, D. Remue, *Appl. Catal. A* **2000**, 204, 19.
68. F. Buciuman, B. Kraushaar-Czarnetzki, *Catal. Today* **2001**, 69, 337.

69. R.S. Besser, W.C. Shin, *J. Vac. Sci. Technol. B* **2003**, *21(2)*, 781.
70. H.Y. Wang, R.S. Foote, S.C. Jacobson, J.H. Schneibel, J.M. Ramsey, *Sens. and Actuators B* **1997**, *45*, 199.
71. S. Wiechel, R. de Reus, M. Lindahl, *Sens. and Actuators A* **1998**, *70*, 179.

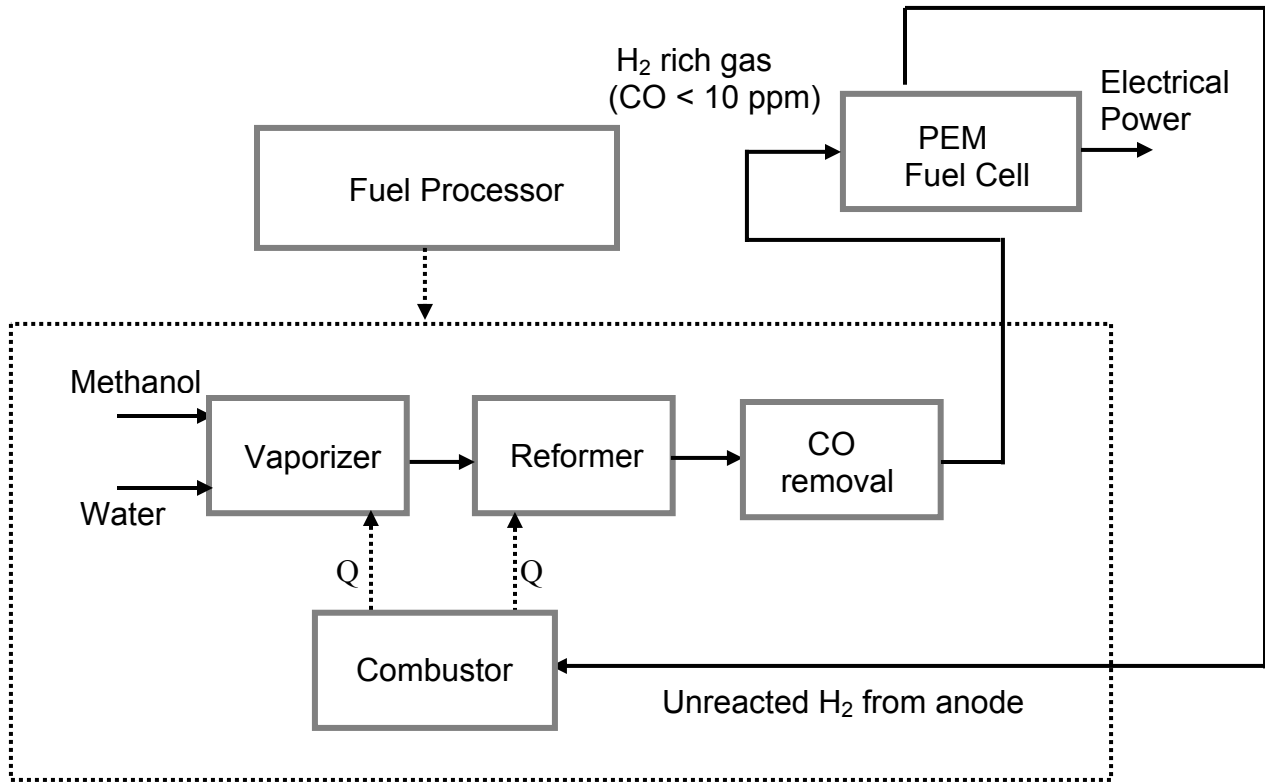


Figure 1

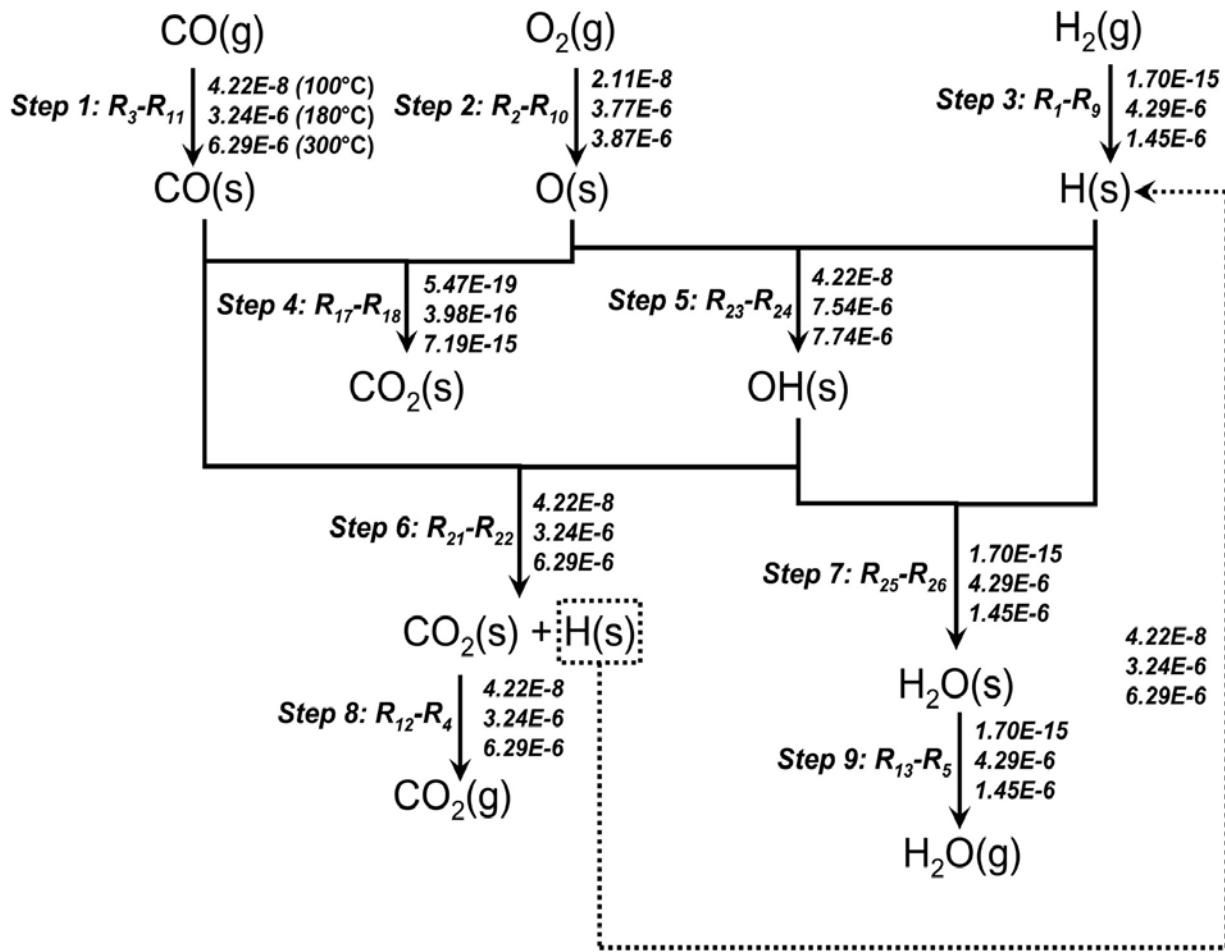


Figure 2

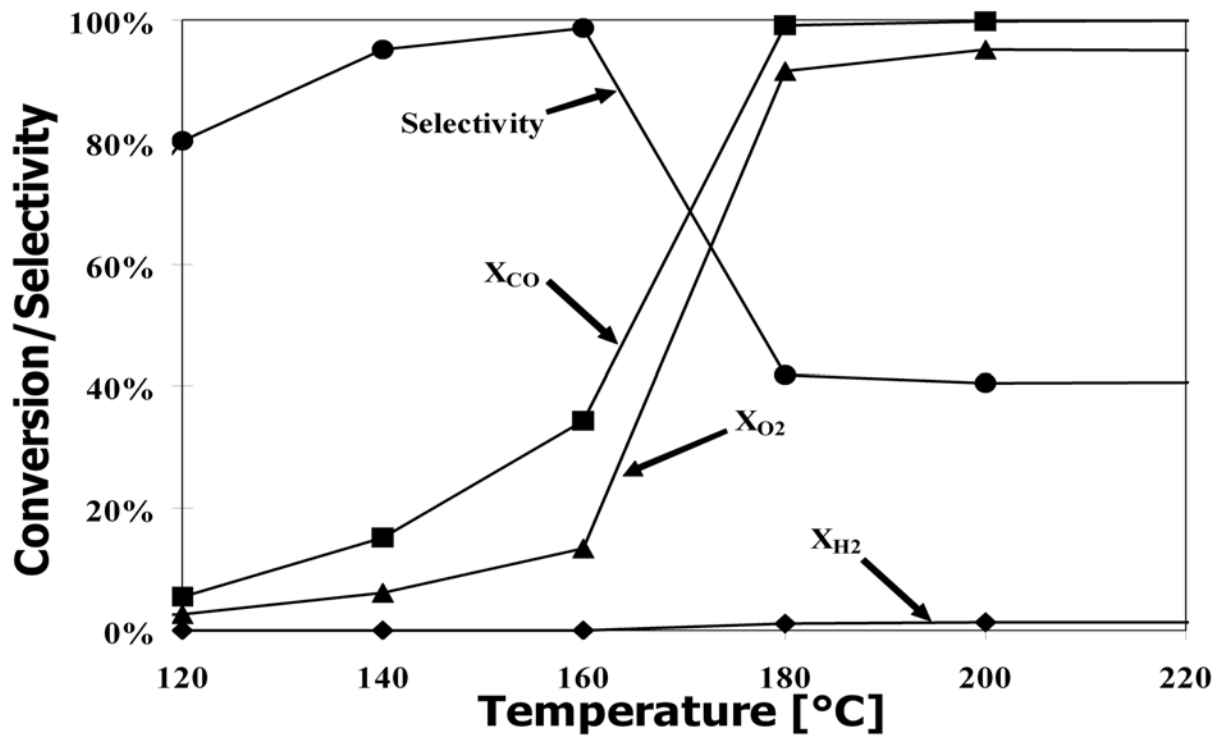


Figure 3

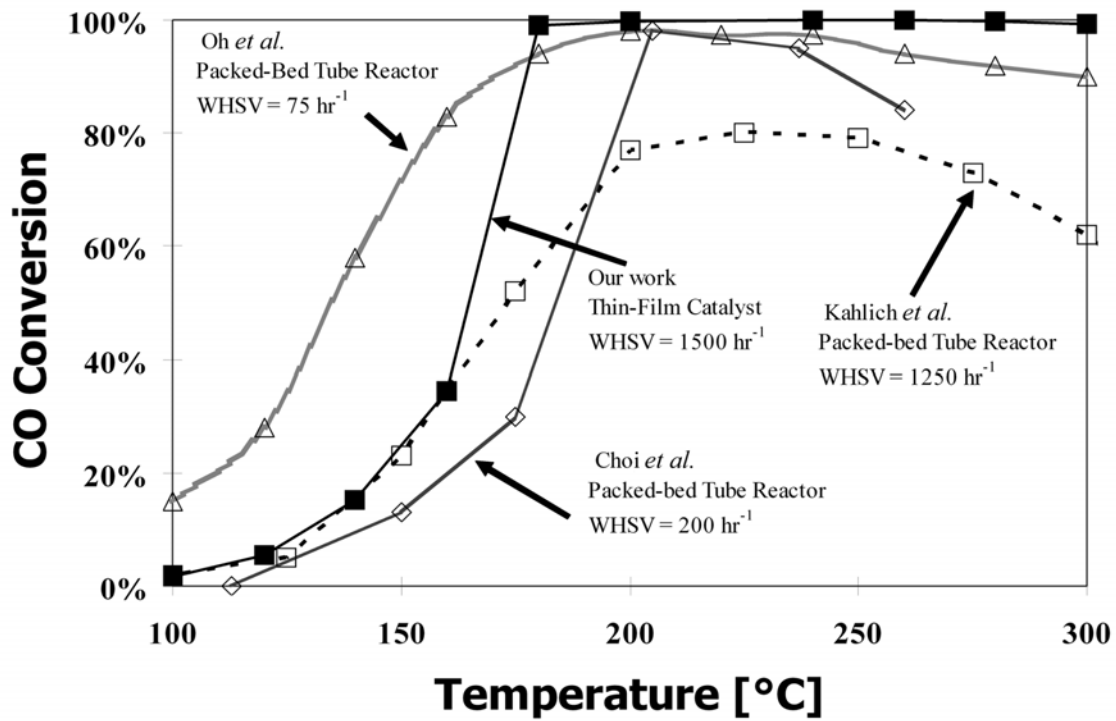


Figure 4

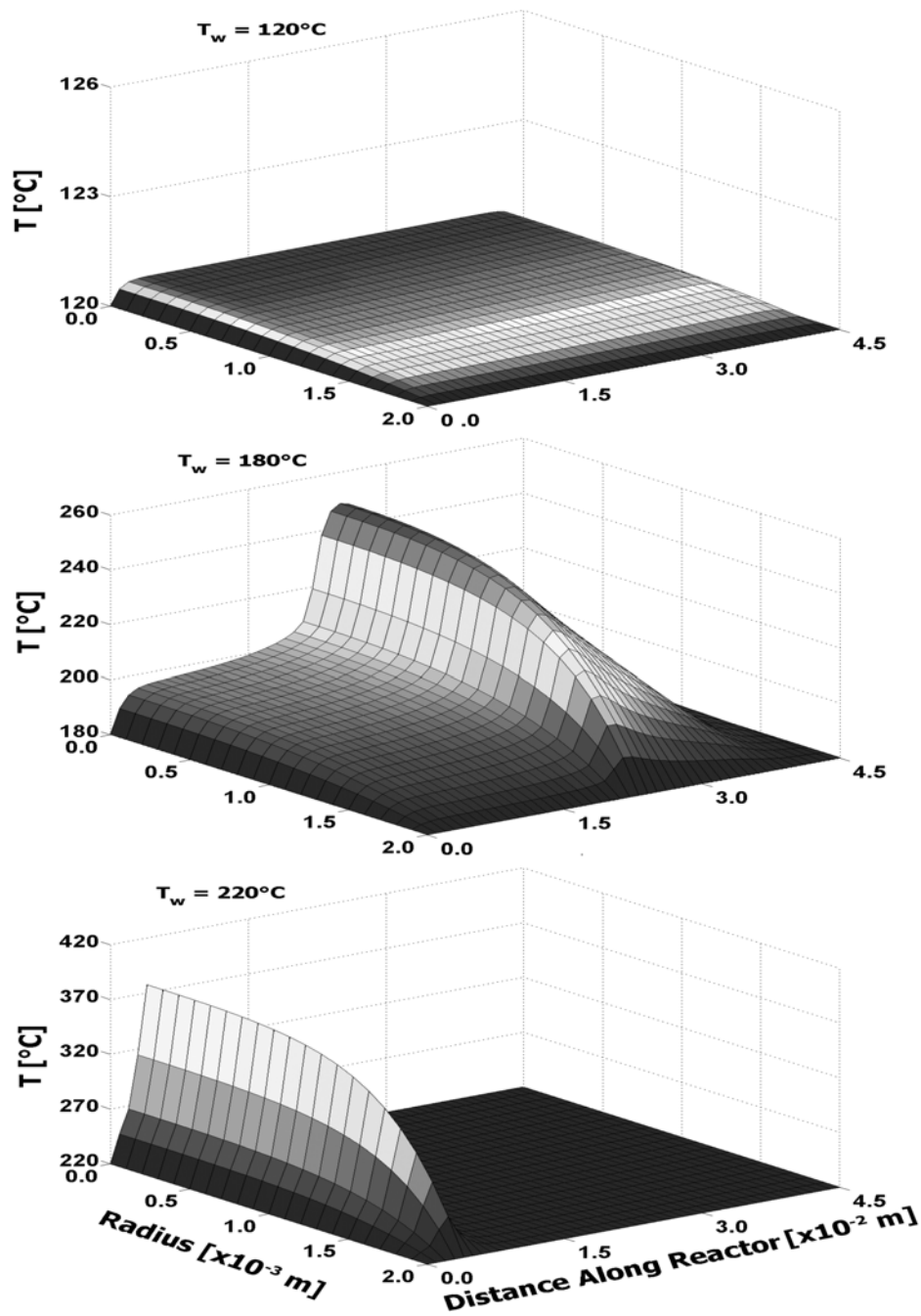


Figure 5

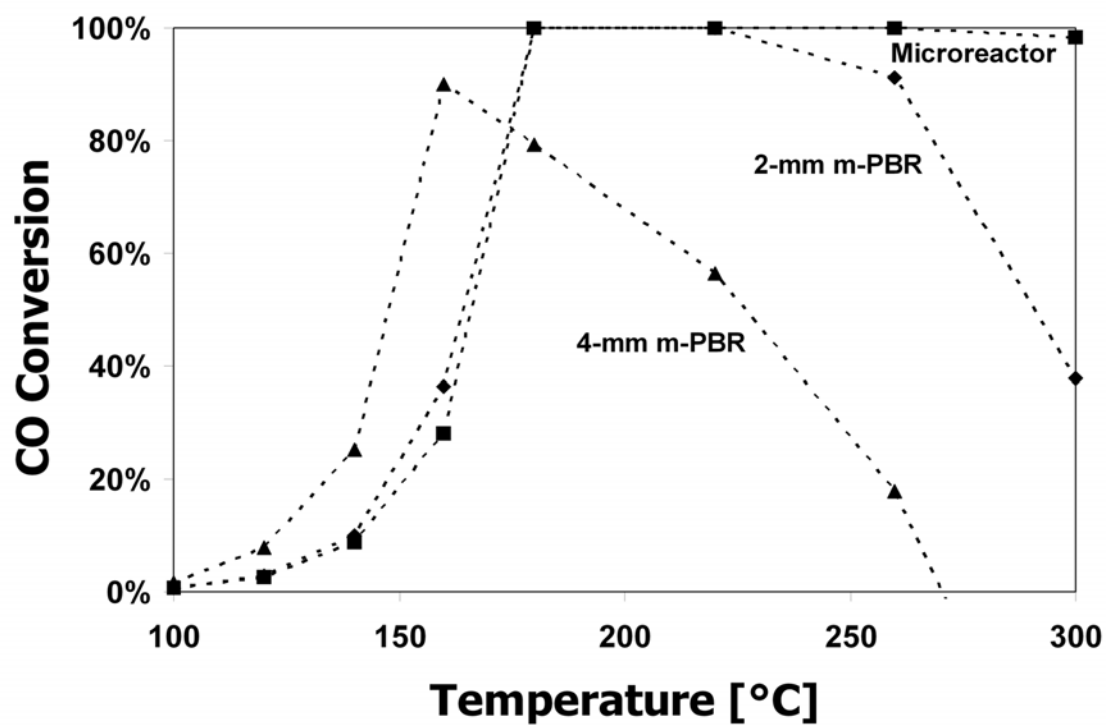
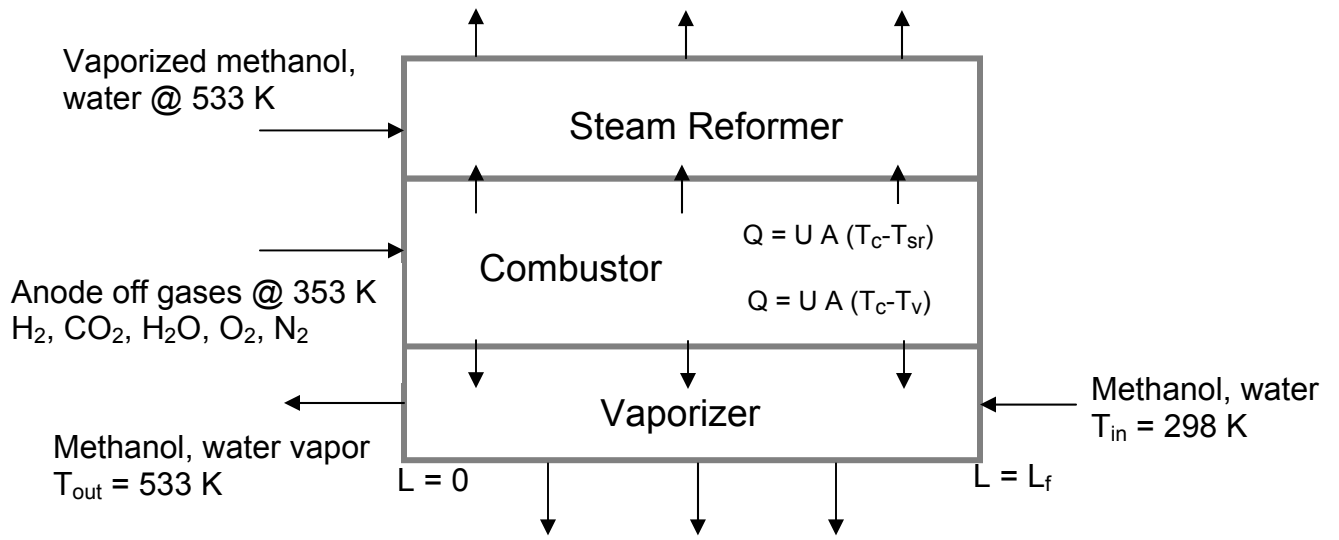
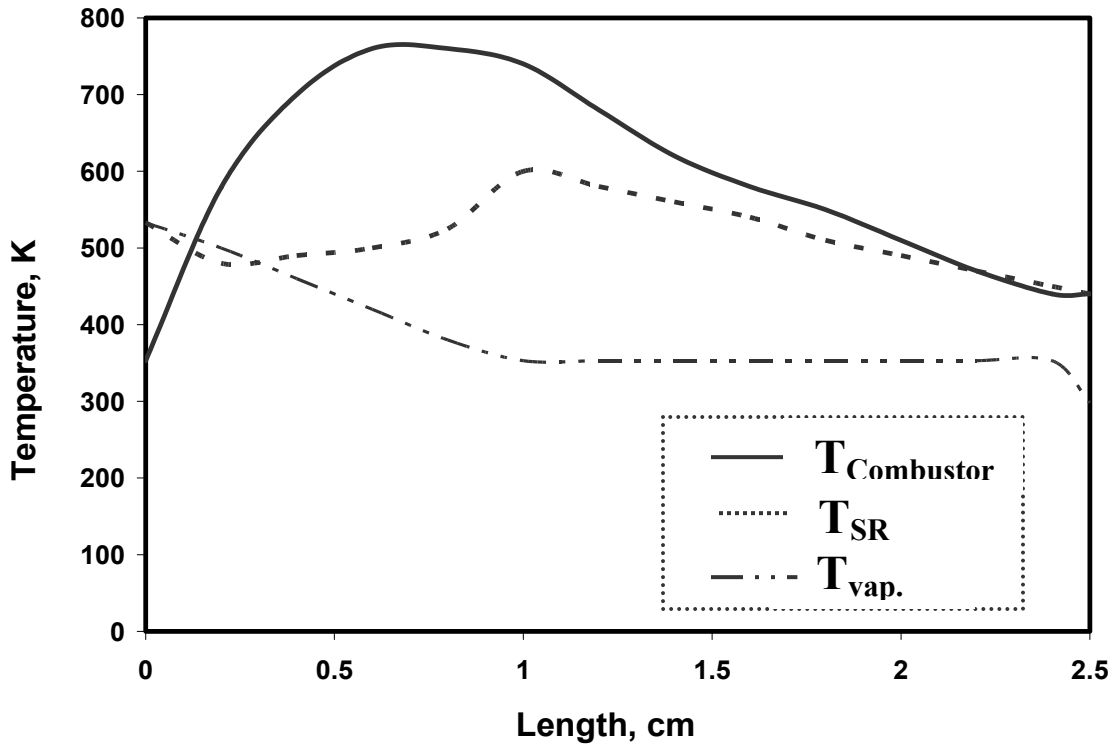


Figure 6



(a)



(b)

Figure 7

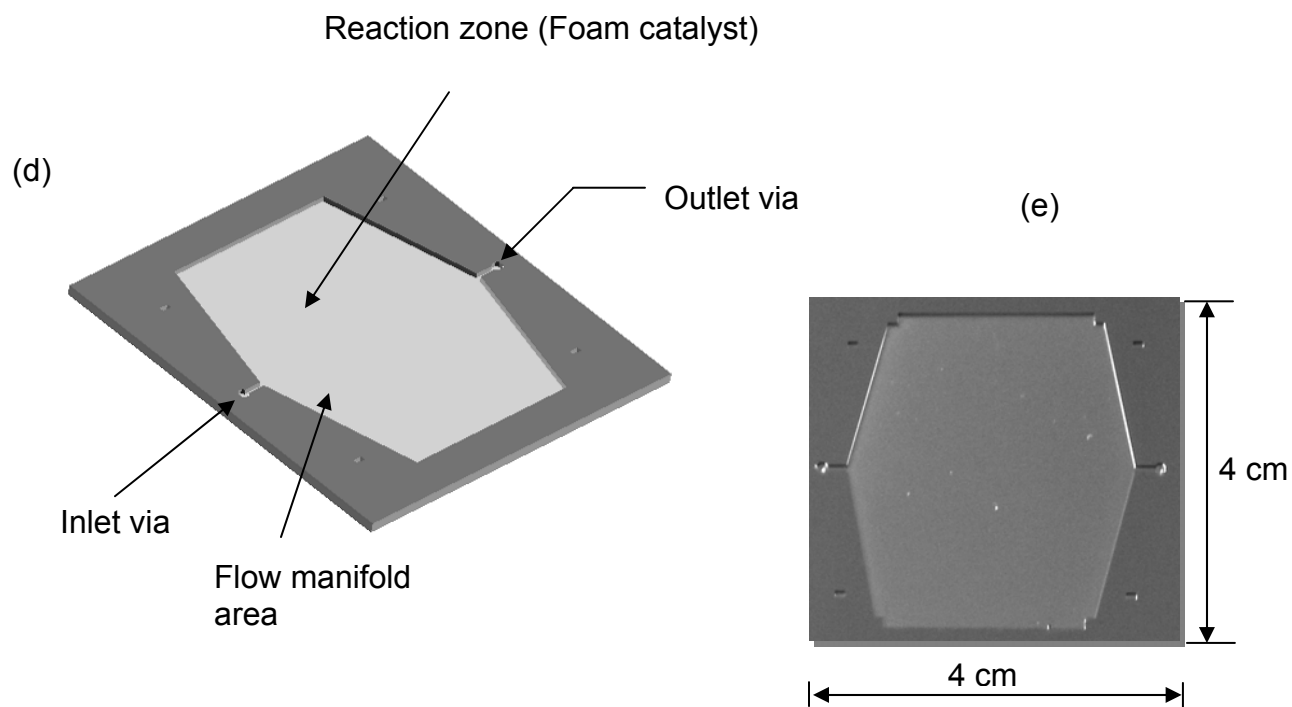
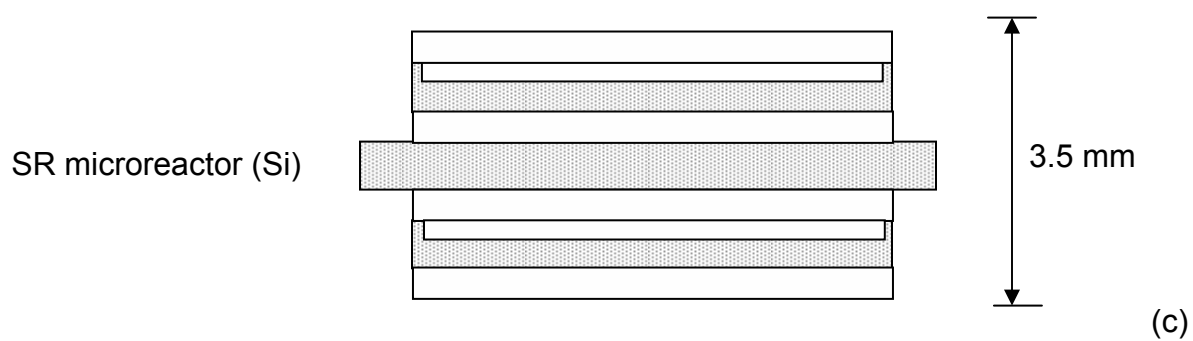
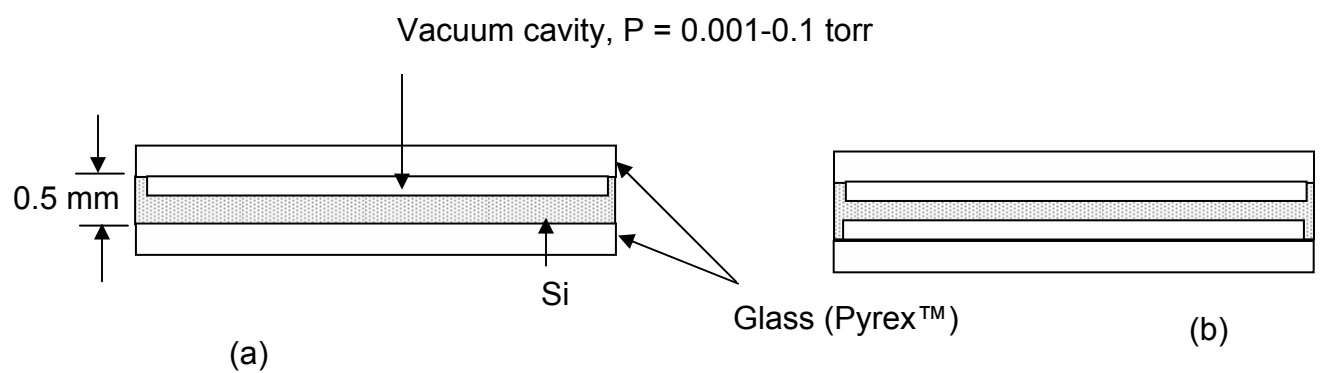


Figure 8

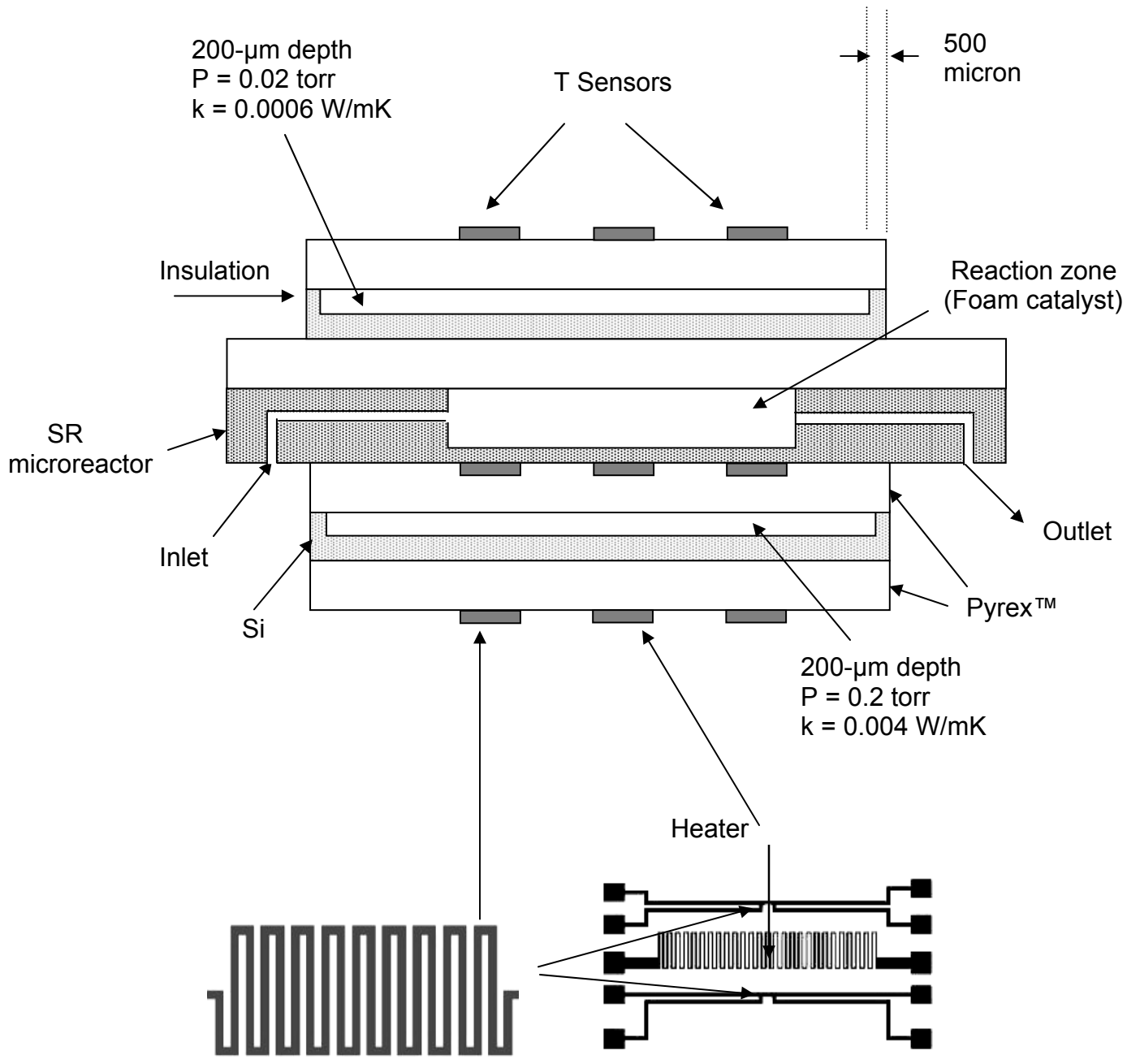
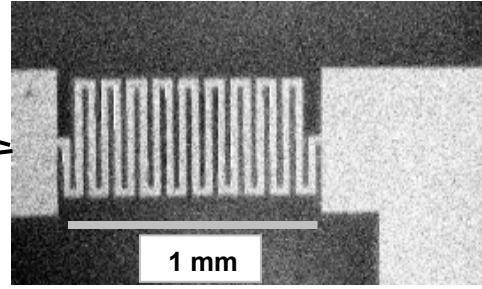
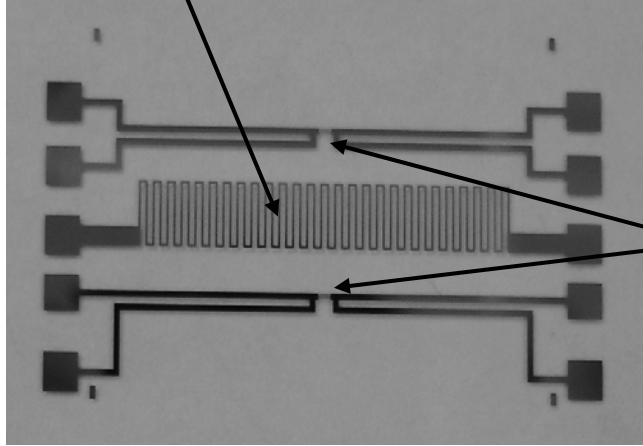


Figure 9

Pt thin film heater



Pt temperature Sensor

Figure 10